

(2)

COMPONENT PART NOTICE

THIS PAPER IS A COMPONENT PART OF THE FOLLOWING COMPILATION REPORT:

TITLE: The Aerospace Environment at High Altitudes and Its Implications for Spacecraft Charging and Communications. Conference Proceedings of Electromagnetic Wave Propagation Panel Symposium Held in The Hague, The Netherlands on 2-6 June 1986.

TO ORDER THE COMPLETE COMPILATION REPORT, USE AD-A185 880 -1.

THE COMPONENT PART IS PROVIDED HERE TO ALLOW USERS ACCESS TO INDIVIDUALLY AUTHORED SECTIONS OF PROCEEDINGS, ANNALS, SYMPOSIA, ETC. HOWEVER, THE COMPONENT SHOULD BE CONSIDERED WITHIN THE CONTEXT OF THE OVERALL COMPILATION REPORT AND NOT AS A STAND-ALONE TECHNICAL REPORT.

THE FOLLOWING COMPONENT PART NUMBERS COMprise THE COMPILATION REPORT:

AD#: P005 692 thru P005 713 = 22

AD#: _____ AD#: _____

AD#: _____ AD#: _____ Total - 23



Accession For	
NTIS	CRA&I
DTIC TAB	<input checked="" type="checkbox"/>
Unannounced	<input type="checkbox"/>
Justification	
By _____	
Distribution / _____	
Availability Codes	
Dist	Avail and/or Special
A7	

DTIC FORM 463
MAR 85

OPI: DTIC-TID

AD-POC5703



Secondary Electron Generation, Emission and Transport: Effects on Spacecraft Charging and NASCAP Models

Ira Katz, Myron Mandell
S-CUBED
P.O. Box 1620
La Jolla, California 92038-1620

James C. Roche, Carolyn Purvis
National Aeronautics and Space Administration
Lewis Research Center
2100 Brookpark Road
Cleveland, Ohio 44135
USA

SUMMARY

Secondary electrons control a spacecraft's response to a plasma environment. To accurately simulate spacecraft charging, the NASA Charging Analyzer Program (NASCAP) has mathematical models of the generation, emission and transport of secondary electrons. This paper discusses the importance of each of the processes and the physical basis for each of the NASCAP models. Calculations are presented which show that the NASCAP formulations are in good agreement with both laboratory and space experiments.

INTRODUCTION

It has long been recognized that the ratio of secondary electrons to incident electrons is a determining factor in spacecraft charging. Experience gained during development of the NASA Charging Analyzer Program (NASCAP) shows that the physical mechanisms which control the generation, emission and transport of secondary and photoelectrons dominate the charging process. This paper addresses three specific aspects of the NASCAP model and discusses the importance of each. The first is the model for generation of secondary electrons as a function of the incident electron angle and energy. The secondary yield for electrons with energies greater than 10 keV is more accurately calculated by NASCAP than by analytical formulas with exponential decay at high energy. This is shown to be very important in understanding the energy of the magnetospheric electron energy spectrum which cause charging. Second, NASCAP models the three dimensional electric fields and potentials around a satellite. Secondary electrons typically have energies of just a few electron volts, and their motion is influenced by weak electric fields. Calculations and experiments have shown that charging on one part of a satellite can cause electric fields which suppress secondary electron emission on other parts of the satellite. This results in overall charging of the satellite even though secondary yields exceed the incident electron current. This phenomenon is inherently multi-dimensional, and its understanding requires the three-dimensional capabilities of NASCAP. Third, just as electric fields can suppress the emission of secondary electrons, they can also transport them from surface to surface. While not of great importance for geosynchronous spacecraft charging, surface transport of secondary electrons dominates the collection of electrons by high voltage spacecraft in Low Earth Orbit. The model of secondary transport in NASCAP/LEO includes the interplay between electric fields parallel and perpendicular to spacecraft surfaces. Comparison with ground and flight data show that secondary electron transport can increase the effective collection area by orders of magnitude.

The NASA Charging Analyzer Program

The NASA Charging Analyzer Program (NASCAP) was developed by S-CUBED under contract to the National Aeronautics and Space Administration to perform dynamic, fully three-dimensional simulations of the charging of a spacecraft in geosynchronous orbit. NASCAP also simulates laboratory experiments relevant to such charging. The various capabilities of NASCAP are described in detail elsewhere^[1,2]. Briefly, the model provides for a three-dimensional, finite element representation of a spacecraft within a 16x16x32 grid. The spacecraft is assumed to charge due to the accumulation on its surface of electrons and ions from the surrounding plasma. Fluxes of particles with energies greater than -50 keV that are able to penetrate the materials are assumed to be negligible, and the depth of deposition of charge within spacecraft materials is neglected. In addition to the collection of primary electron and ion currents, other surface mechanisms, namely secondary electron emission, backscatter and photoemission, are also included. The distribution of incident particle energies may be Maxwellian, double Maxwellian, or described by a set of tabulated spectral data points. The angular distribution function may be isotropic, or a loss-cone/gain-cone type of anisotropic form.

NASCAP is capable of solving Poisson's equation around a complex three-dimensional object. The object may be composed of cubes, sections of cubes, thin plates and long booms. An easy to use object definition protocol is provided. The computational space may extend as far from the object as desired. Outer boundary conditions may be grounded or monopolar. Under normal usage, space charge is ignored (i.e., Laplace's equation is solved). Optionally, Debye screening may be invoked, or the space charge associated with low energy emitted electrons may be taken into account.

The object may be composed of up to fifteen different conducting segments. Each segment may be held at fixed potential or allowed to float, or segments may be biased relative to one another. The object may be covered by up to fifteen different surface materials. The materials may be conductors or thin insulating layers overlying conductors. The bulk and surface conductivities and the emissive properties of the materials may be user specified, with default values provided.

*This work supported by NASA/Lewis Research Center, Cleveland, Ohio, under Contract NAS3-23881.

A NASCAP simulation consists of a series of 'timesteps.' During each timestep the incident and emitted currents to each surface cell are computed and the surface potentials updated, taking into account bulk and surface conductivity, suppression of secondary electrons, and changes in current during the timestep. Then the space potentials and fields are updated. For simulation of laboratory experiments the incident currents are most commonly computed by tracking charged particles forward from monoenergetic electron and ion guns. For spacecraft simulation, orbit-limited collection from a Maxwellian plasma is most commonly assumed. Various other options are available for each case.

NASCAP has been validated by comparing its predictions to experimental data on charging of material samples^[3], spacecraft instrumentation^[4] and model spacecraft^[5] subject to electron gun irradiation, as well as to actual spacecraft data^[6]. Experience has demonstrated NASCAP to be a useful predictive tool when applied to the rarefied plasma conditions for which it was intended and the physical principles underlying NASCAP have been proved sound.

Secondary Electron Yields

Previous studies by several authors have shown that, for a Maxwellian plasma, charging results only when the electron environment exceeds some threshold temperature.^[7,8] This is because secondary yields typically are greatest for electrons with energies below about 1 keV and are less than unity for electrons with energies above a few keV. Below the threshold, the integral secondary and backscatter yields exceed the incident electron flux, so net charging cannot occur.

The concept of an energy below which the electrons do not contribute to charging was put forth by Lai, Gussenoven and Cohen.^[9] Both the study by Laframboise and that by Lai indicated charging threshold temperatures of a few keV and that charging was caused by electrons with energies the order of 10 keV. Those energies are about a factor of three lower than seen in the SCATHA survey^[10]. A recent study^[11] has shown that this discrepancy occurs because the formulation of secondary yields used by these authors was inaccurate and predicted unphysically small secondary yields for electrons in the relevant energy range (5-50 keV).

Theory^[12] and experiment^[13] confirm that secondary yield is proportional to stopping power for high energy incident electrons. Using secondary formulations which are more correct at high energy, such as those from NASCAP^[2,14], or that suggested by Burke^[15], the mean energy of the electrons which charge a satellite agrees with the SCATHA observation that electrons above 30 keV caused spacecraft charging^[10].

Typical yield of secondary electrons as a function of energy is shown in Figure 1. The yield is proportional to the energy deposited by the incident electron in the top 20-100 angstroms of the material. For low energy electrons (with range comparable to or less than this distance) the yield is proportional to the particle energy. At high energy the yield is proportional to the stopping power. This behavior has both a strong theoretical basis and has been verified experimentally.^[13] The maximum yield occurs in the transition between these two regimes, which is at a few hundred volts for most materials. For spacecraft charging purposes it is important to have a reasonable estimate of secondary yields for 5-50 keV primary electrons. For most materials the electron range is well-represented in this energy regime by a power law:

$$\text{Range} = \text{Constant} \times \text{Energy}^p \quad (1)$$

with $1.5 < p < 2.0$. Since

$$\text{Stopping Power} = [d(\text{Range})/d(\text{Energy})]^{-1} \quad (2)$$

we expect secondary yield to fall off inversely (or slower) with respect to the energy of the primary electron:

$$Y(E) = [E/E_{\text{ext}}]^{1-p} \quad (3)$$

where E_{ext} is the energy at which the secondary yield extrapolates to unity. (This is equivalent to the form suggested by Burke^[15].) Proposed simplified formulas^[16,17] having exponential falloffs, while easy to use analytically, will invariably underestimate the yield of secondary electrons for environments capable of charging spacecraft. For most spacecraft materials (which have low atomic number) backscatter yields increase monotonically with energy from zero to few tenths.

Following Lai et al.,^[9] E_{upper} is defined as the energy below which electrons do no charging, i.e.,

$$\int_0^{E_{\text{upper}}} E \exp(-E/\theta) [1-Y(E)-B(E)] dE = 0 \quad (4)$$

The parameter E_{upper} is a function of θ , being undefined for θ below the charging threshold, infinite at threshold, and reaching a finite limit as $\theta \rightarrow \infty$.

Using the secondary emission formulation found in NASCAP gives a value of 31.2 keV for E_{upper} . This contrasts with the 11.1 keV value reported by Lai et al.^[9]. The threshold Maxwellian temperature for charging is found by NASCAP to be 14.0 keV, compared with 4.9 keV from Lai. The low values reported by Lai are entirely due to the inadequacy of the secondary formulation used.

For the purpose of comparison with data from the SCATHA satellite, the material properties are taken to be those of solar cell cover slips, since most of the exterior surface of the spacecraft is covered with solar cells. (The results would change little for most typical spacecraft coverings such as teflon beta cloth.) The dashed curve in Figure 2 shows the dependence of E_{upper} (calculated by NASCAP) with the temperature of the ambient environment. The high temperature limiting value of E_{upper} is 15.1 keV, and the threshold temperature is 6.8 keV. These are much lower than those for Gold, which has a higher atomic number, and therefore higher secondary and backscatter yields. We can define as well the mean energy of electrons which cause charging as

$$E_{charging} = \frac{\int_{E_{upper}}^{\infty} E^2 \exp(-E/\theta) [1-Y(E)-B(E)] dE}{\int_{E_{upper}}^{\infty} E \exp(-E/\theta) [1-Y(E)-B(E)] dE} \quad (5)$$

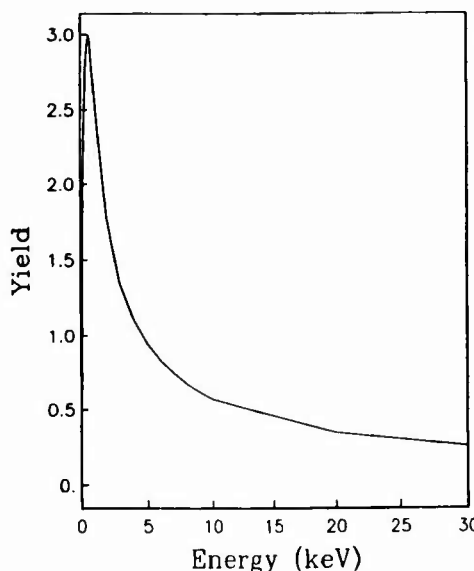


Figure 1. Secondary yield vs. primary electron energy for solar cell coverslip material, assuming isotropic incidence.

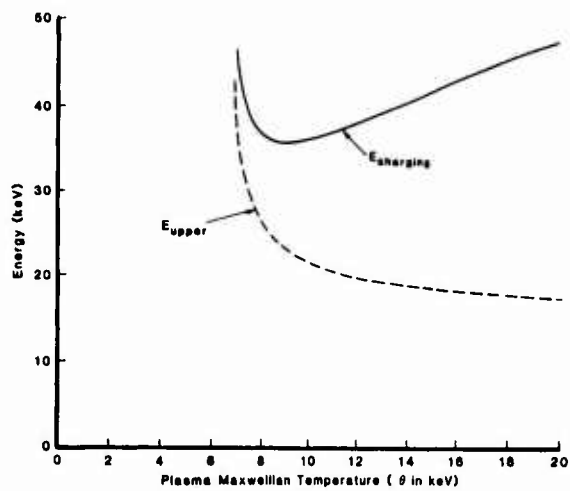


Figure 2. E_{upper} (dashed curve) and $E_{charging}$ (solid curve) as functions of assumed Maxwellian temperature.

The solid curve in Figure 2 shows the dependence of this value on temperature. Unlike E_{upper} , the average value has a minimum near the threshold temperature. For the SCATHA materials the minimum value is 35 keV in agreement with observation. The flux of electrons with energies greater than E_{upper} and within θ of the $E_{charging}$ contribute most of the net electron current to the surface and should be a reliable indicator of charging.

Electric Field Limiting of Secondary and Photo Electron Emission

The sheath of low-energy electrons which can form near a charged surface is known to have complex structure. NASCAP has the capability of determining low energy electron currents through tracking of emitted particles. However, not only is such a procedure time-consuming, but it jeopardizes the numerical stability of the calculation. This is because these currents are sensitive to surface potential changes comparable to the two-volt characteristic energy of emitted electrons, much smaller than the kilovolt differential potentials of interest. Mandell et al [2] showed that any substantial electric field can dominate space charge effects in determining photosheath structure. It then follows that the surface potential will attain a value such that the fraction of secondary or photoelectrons escaping over an electric field barrier is just that needed to maintain current balance.

Consider space charge-limited emission in the presence of an external field. If the field is negative (i.e., into the surface) no sheath will form, so only positive fields will be considered. For the simple case of monoenergetic (energy E) electrons emitted normally from a plane surface, a virtual cathode will form at a distance d from the surface. The sheath thickness d is found using the space charge equation [19].

$$\left(\frac{dV}{dx} \right)^2 = \left(\frac{dV}{dx} \right)_{x=d}^2 - \frac{8J}{\epsilon_0} \left(\frac{mV}{2|e|} \right)^{1/2} \quad (6)$$

with the boundary condition

$$V(d) = 0$$

$$V(0) = E/|e|$$

$$\left(\frac{dV}{dx} \right)_{x=d} = \text{external field}$$

Figure 3 shows the sheath thickness as a function of external field for the parameters $J = 3 \text{ nA/cm}^2$ and $E = 2 \text{ eV}$. It is apparent that any substantial positive external field will completely dominate space charge effects and suppress emission of low energy electrons. Taking into account the distributed spectrum of low-energy emitted electrons, this leads to the following principle:

Under conditions of strong differential charging a photoemitting surface will reach a potential such as to maintain a positive external electric field of a few volts per meter.

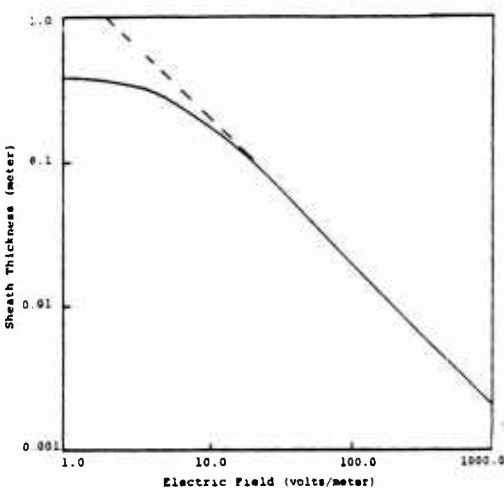


Figure 3. Electron sheath thickness outside a planar surface emitting 2 eV electrons as a function of electric field in the low current limit (dashed line) and for 3 nA/cm^2 emitted current (solid curve).

The precise value of this field is determined by the requirement that the unsuppressed high energy tail of the photoemission spectrum maintain current balance.

NASCAP was run to calculate the electrostatic potentials on the surface of, and in the space surrounding, a sunlit teflon-coated sphere. Currents to the sunlit surfaces were determined based on the principle put forth in the previous section. From an initial uncharged state, the sphere reached a final steady state having 2.5 kV of differential charging. Figure 4 shows the potentials on a shaded and a sunlit surface cell as a function of time.

Figures 5-9 show the time development of the electrostatic field. (The satellite-sun line lies in the plane of these figures. Dark and sunlit cells are differentiated by shading.)

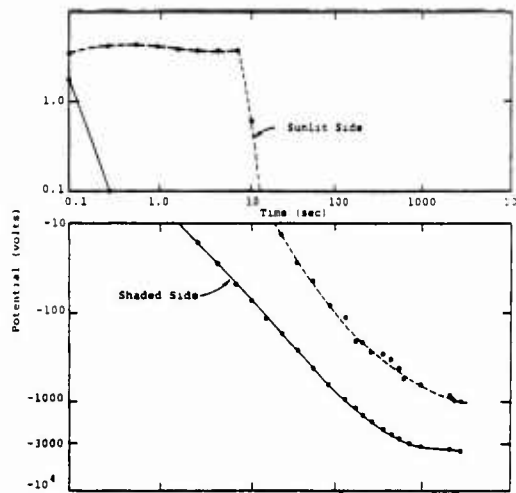


Figure 4. Potentials on shadowed and solar illuminated surfaces of a teflon sphere in a plasma ($N_e = 10^6/m^3$, $\theta = 20$ keV).

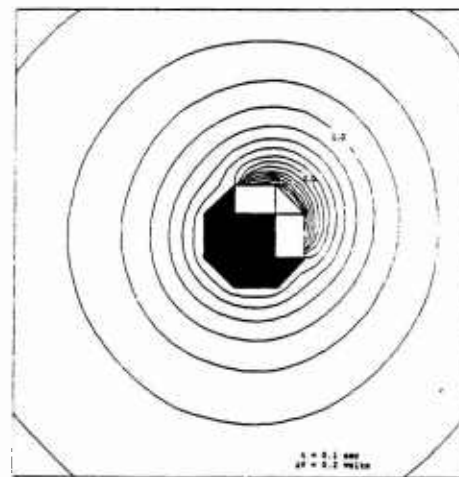


Figure 5. Potential contours about a sunlit sphere early in time.

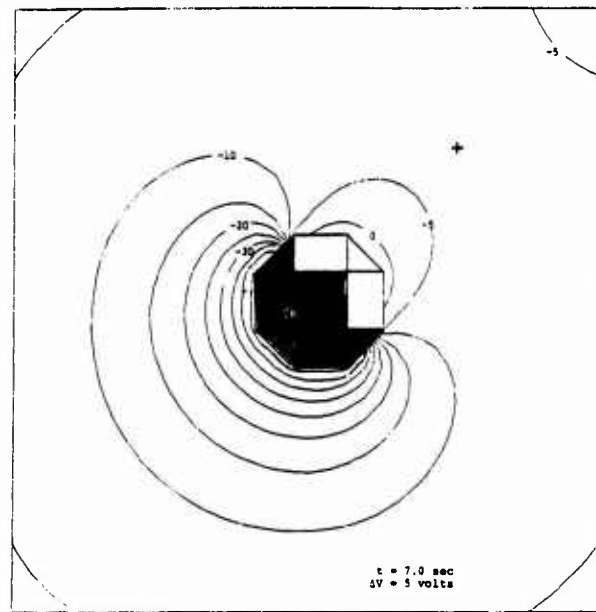


Figure 6. Potential contours around sunlit sphere showing early appearance of saddle point (x) at -5.6 volts.

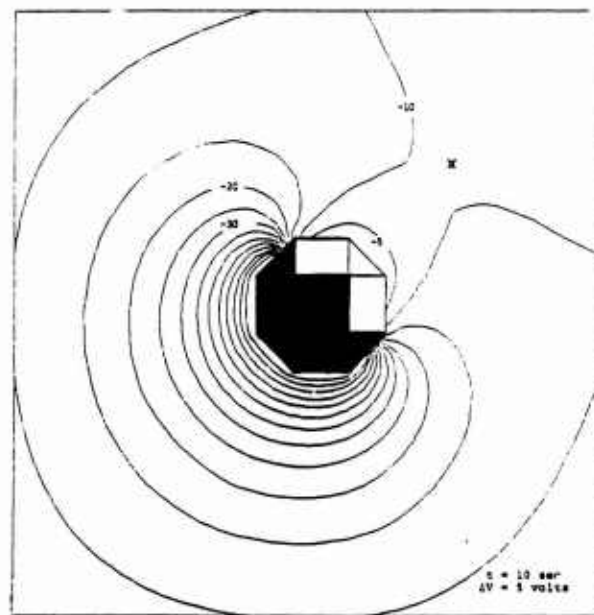


Figure 7. Potential contours around sunlit sphere showing fully formed saddle point at approximately -8 volts.

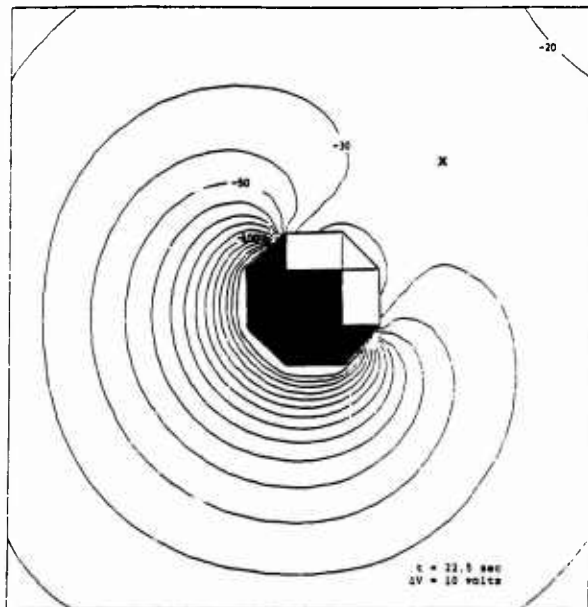


Figure 8. Potential contours about sunlit sphere showing saddle point at approximately -25 volts.

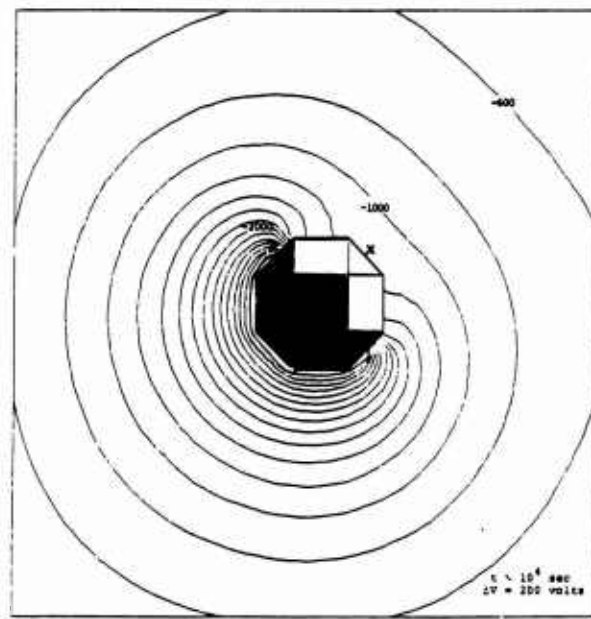


Figure 9. Steady state potential contours about sunlit sphere.

For the first -0.1 seconds the sphere charged uniformly (Figure 5). Over the next few seconds, the negative charge accumulated by the shaded surfaces began to dominate the electrostatic field, causing a saddle point to appear in front of a sunlit surface (Figures 6-7). At about 10 seconds the potential at the saddle point became negative. In accordance with the principle put forth above the sunlit surface maintained a potential a few volts positive relative to the saddle point (Figure 8). Final steady state (Figure 9) is reached with the sunlit surface at -1.0 kV and the shaded surface at -3.6 kV.

Secondary Electron Transport in NASCAP/LEO

NASCAP/LEO [20,21] is a computer code designed to study the interaction between a high-voltage spacecraft and a short Debye length plasma. In particular, NASCAP/LEO predicts the electrostatic potential on insulating surfaces and in the surrounding plasma, and the parasitic current driven through the plasma. The kernel of NASCAP/LEO is the electrostatic potential solver, which solves a nonlinear Poisson-like equation with either potential or electric field boundary conditions at each surface cell. Two features of particular interest here are the local subdivision capability, and the treatment of secondary electron conductivity as an electric field boundary condition.

NASCAP/LEO geometry consists of an object contained within a "primary grid" (usually 17x17x33 grid points) which may be contained within "outer grids" having successively double the physical spacing. The local subdivision capability allows the modeling of small but important object features within the primary grid.

When the low-energy electrons are emitted and re-attracted by a surface, they form an effective surface conducting layer, [22,23] with surface conductivity, $\sigma_{||}$ [ohms⁻¹] given by

$$\sigma_{||} = (4/E_{\perp}^2) \langle \epsilon \rangle (Y J_{in}) \quad (7)$$

Here E_{\perp} is the electric field component normal to the surface, $\langle \epsilon \rangle$ is the mean energy of emitted electrons (eV), and $(Y J_{in})$ is the current density of emitted electrons. If electrons are emitted as a result of an incident electron current J_{in} with secondary yield Y , two-dimensional current balance requires

$$J_{in} = Y \cdot (\sigma_{||} E_{||}) \quad (8)$$

where $E_{||}$ is the tangential electric field. If we make the approximation that $\sigma_{||}$ can be taken outside the divergence, equations (7) and (8) combine to give

$$E_{\perp} = [4 \langle \epsilon \rangle Y E_{||}]^{1/2} \quad (9)$$

NASCAP/LEO applies equation (9) self-consistently to insulating surfaces where secondary emission dominates. When secondary emission does not dominate, surfaces charge straightforwardly to reach current balance. In the planar, absorbing approximation, such surfaces reach a negative potential given by

$$V = (\theta/2) \ln(m_e/m_i) \quad (10)$$

where θ is the plasma temperature (eV).

These concepts were used to model [24] measurements of plasma sheath potentials by Gabriel, Garner and Kitamura. [25] The experimenters measured the plasma potential as a function of distance from the sample along the pinhole axis.

Under negative bias, there is no secondary electron conductivity mechanism, as all secondary electrons escape. For a 0.64 cm diameter pinhole biased to -452 volts, both calculation and experiment (Figure 10) showed the potential drop below 20 volts by a distance of 1 cm from the surface.

For the same pinhole biased to +458 volts, both calculation and experiment (Figure 11) showed potentials of 60 volts or more at the same one centimeter point. The calculations predicted the surface to be charged to substantial positive potentials to a radius exceeding one centimeter. While the surface potentials were not measured in this set of experiments, the effect was observed in earlier experiments by Stevens et al. [26] In both sets of experiments, the spread of positive potentials onto the insulator surrounding a simulated pinhole led to a vast increase in the collected electron current, which was well simulated by NASCAP/LEO.

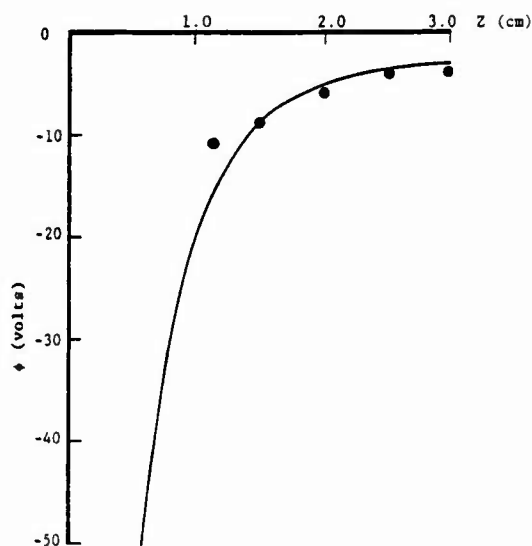


Figure 10. Potentials on axis for 0.64 cm diameter pinhole at -452 V.
Solid line: Calculated with kapton at volts; Points: Experiment.

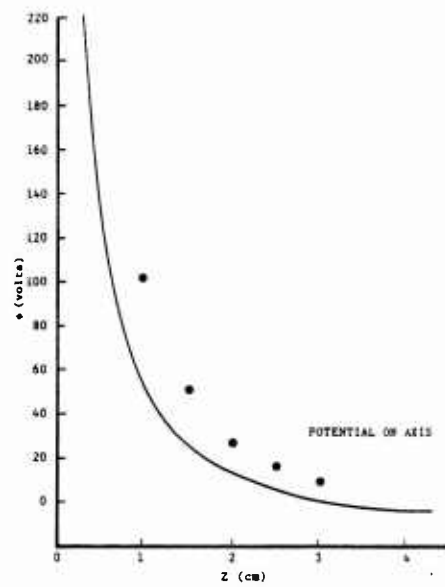


Figure 11. Potentials for 0.64 cm diameter pinhole. Upper solid curve:
Calculated for 458 V bias. Points: Experiment for 458 V bias.

Conclusions

Secondary electron phenomena play an important role in many aspects of spacecraft charging. In this paper three distinct cases were discussed that show:

- (1) A good formulation for the secondary electron yield as a function of incident electron energy is needed in order to determine whether a given particle spectrum will cause strong negative charging for a given spacecraft material;
- (2) Suppression of secondary electron emission by electric fields plays a dominant role in sunlight charging; and
- (3) Surface conductivity associated with the presence of a secondary electron layer plays a key role in enhancing the current collection by small, positively biased pinholes or interconnects.

The treatments of these various aspects of secondary electron phenomena in the NASCAP and NASCAP/LEO codes provide good quantitative results for secondary electron effects. Errors are probably due more to uncertainties in the input parameters to the codes and to uncertainties in experimental measurements than to inadequacies in the code formulations. In developing these treatments we have not merely generated a complex computer model, but also gained a better qualitative understanding of the role of low energy emitted electrons in spacecraft-plasma interactions.

References

1. Katz, I., J. J. Cassidy, M. J. Mandell, G. W. Schnuelle, P. G. Steen, and J. C. Roche, "The Capabilities of the NASA Charging Analyzer Program", Spacecraft Charging Technology - 1978, NASA CP 2071, AFGL-TR-79-0082, pp. 101-122 (1979).
2. Mandell, M. J., P. R. Stannard, and I. Katz, NASCAP Programmer's Reference Manual, S-CUBED Report SSS-84-6638 (1984).
3. Roche, J. C., and C. K. Purvis, "Comparison of NASCAP Predictions with Experimental Data", Spacecraft Charging Technology - 1978, NASA CP 2071, AFGL-TR-79-0082, pp. 144- 157, (1979).
4. Purvis, C. K. and J. V. Staskus, "SCATHA SSPM Charging Response: NASCAP Predictions Compared with Data", Spacecraft Charging Technology - 1980, NASA CP 2182, AFGL-TR-81-0270, pp. 592-607, (1981).
5. Staskus, J. V., and J. C. Roche, "Testing of a Spacecraft Model in a Combined Environment Simulator", IEEE Transactions on Nuclear Science NS-28, pp. 4509-4512 (1981).
6. Katz, I., P. R. Stannard, L. Gedeon, J. C. Roche, A. G. Rubin, and M. F. Tautz, "NASCAP Simulations of Spacecraft Charging of the SCATHA Satellite", Spacecraft/Plasma Interactions and their Influence on Field and Particle Measurements, ESA SP-198, pp. 109-114, (1983).
7. Stannard, P. R., F. W. Schnuelle, I. Katz, and M. J. Mandell, "Representation and Material Charging Response of GEO Plasma Environments" Spacecraft Charging Technology - 1980, NASA CP 2182, AFGL-TR-81-0270, pp. 560-579, (1981).
8. Laframboise, J. G., and M. Kamituma, "The Threshold Temperature Effect in High-Voltage Spacecraft Charging", Proceedings of the Air Force Geophysics Laboratory Workshop on Natural Charging of Large Space Structures in Near Earth Polar Orbit: 14-15 September 1982, AFGL-TR-83-0046, pp. 293-308, (1983).
9. Lai, S. T., M. S. Gussenoven and H. A. Cohen, "The Concepts of Critical Temperature and Energy Cutoff of Ambient Electrons in High Voltage Charging of Spacecraft", Proceedings of the 17th ESLAB Symposium on Spacecraft/Plasma Interactions and their Influence on Field and Particle Measurements, Noordwijk, The Netherlands, 13-16 Sept. 1983, ESA SP-198, pp. 169-175, (1983).
10. Mullen, E.G., M. S. Gussenoven, D. A. Hardy, T. A. Aggson, B. G. Ledley and E. Whipple, "SCATHA Survey of High Level Spacecraft Charging in Sunlight". (To be published).
11. Katz, I., M. J. Mandell, G. Jongeward, M. S. Gussenoven, "The Importance of Accurate Secondary Electron Yields in Modeling Spacecraft Charging", (To be published).
12. Alig, R. C., and S. Bloom, "Secondary-Electron-Escape Probabilities", Journal of Applied Physics 49, 3476-3480, (1978).
13. Kanter, H., "Energy Dissipation and Secondary Electron Emission in Solids", Physical Review 121, 677 (1961).
14. Katz, I., D. E. Parks, M. J. Mandell, J. M. Harvey, D. H. Brownell, S. S. Wang, M. Rotenberg, A Three Dimensional Dynamic Study of Electrostatic Charging in Materials, NASA CR-135256, S-CUBED Report SSS-R-77-3367, (1977).
15. Burke, E. A., "Secondary Emission from Polymers" IEEE Transactions on Nuclear Science NS-27, 1760-1764, (1980).
16. Sanders, N. L. and G. T. Inouye, "Secondary Emission Effects on Spacecraft Charging: Energy Distribution Consideration", Spacecraft Charging Technology-1978 NASA CP- 2071, AFGL-TR-79-0082, pp. 747-755, (1979).
18. Sternglass, E. J., Physical Review 95, 345-358 (1954).
19. Page, L. and N. Adams, Principles of Electricity, Princeton: Van Nostrand, 253, (1958).
20. Mandell, M. J., I. Katz and D. L. Cocke, "Potentials on Large Spacecraft in LEO", IEEE Transactions on Nuclear Science NS-29, pp. 1584-1588, (1982).
21. Katz, I., M. J. Mandell, G. W. Schnuelle, D. E. Parks and P. G. Steen, "Plasma Collection by High-Voltage Spacecraft at Low Earth Orbit", Journal of Spacecraft and Rockets 18, 79, (1981).
22. Mandell, M. J., I. Katz and G. W. Schnuelle, "Photoelectron Charge Density and Transport near Differentially Charged Spacecraft", IEEE Transactions on Nuclear Science NS-26, p. 5107 (1979).
23. Pelizzari, M. A. and D. R. Criswell, "Differential Photoelectric Charging of Nonconducting Surfaces in Space", Journal of Geophysical Research 83, p. 5233 (1978).
24. Mandell, M. J and I. Katz, "Potentials in a Plasma over a Biased Pinhole", IEEE Transactions on Nuclear Science NS-30, 4307-4310 (1983).

25. Gabriel, S. B., C. E. Garner and S. Kitamura, "Experimental Measurements of the Plasma Sheath Around Pinhole Defects in a Simulated High-Voltage Solar Array," AIAA Paper No. 83-0311, AIAA 21st Aerospace Sciences Meeting, Reno, NV, January 10-13, 1983.

26. Stevens, N. J., F. D. Berkope, C. K. Purvis, N. Grier, and J. Staskus, "Investigation of High Voltage Spacecraft System Interactions with Plasma Environments," AIAA Paper 78-672, April, 1978.

DISCUSSION

D.K.Davies,UK

Does the NASCAP model include details of particle-surface interactions such as the dependence of electron generation on incident ion dynamics? Are processes such as Auger neutralisation, for example, modelled?

Author's Reply

Particle-surface interactions in NASCAP include ion secondary electron generation as a function of ion energy and angle. The specific mechanism for neutralization and secondary generation is not specified.

D.Verdi,UK

Bulk conduction referred to briefly. What is the magnitude of this contribution for a thin dielectric on a conductive substrate when exposed to sunlight, where photo-conduction will be involved?

Author's Reply

We have such cases for thin (≈ 1 mil) dielectrics where bulk conductivity dominate differentials, other cases where conductivity is negligible and intermediate cases. High energy electron radiation induced conductance plays an important role, and is modelled in NASCAP.

H.Thiemann,GE

Does NASCAP/LEO include any influence of space charges created by secondary electrons or plasma particles to the outer potential distribution?

Author's Reply

NASCAP includes secondary electron space charge as an option, typical barrier heights calculated have not exceeded a few lengths of a volt for SCATHA. For high voltage charging they make no difference.

G.L.Wrenn,UK

You claim that spacecraft charging is controlled by 30 KeV electrons. Is it not true that all electrons with an energy greater than the upper cross-over point of the secondary electron yield curve, about 1 KeV or less, contribute to the charging?

Author's Reply

Following Lai et al, we define the charging electrons as those above the energy such that the surface current integral up to that energy gives Albedo of unity. This is much above the second cross-over.

P.Edenhofer,GE, comment

I found your concluding remarks especially interesting concerning the important influence of low energy electrons on S/C charging. The problem is that, generally, low energy electrons can hardly be measured in situ by scientific satellite payloads since the relevant on-board sensitivity level typically is $\gtrsim 10$ eV (e.g. Giotto). Thus, for taking into account low energy electrons, numerical computations and simulations usually are the only tools to work with.

L.Levy,FR

Are the low potentials measured on this SCATHA OSR's to be explained rather in terms of importance of Sec/emissions or of conductivity? (enhanced conductivity)

Author's Reply

I am unfamiliar with the data.

M.A.Heinemann,US

In low earth orbit, how much effect does the earth's magnetic field have on the hopping conductivity?

Author's Reply

I don't know; I haven't really thought about it.

